Structural study of the effect of mineral additives on the transparency, stability, and aging of silicate gels

N. El Felss, A. Gharzouni, Maggy Colas, J. Cornette, I. Sobrados, S. Rossignol

Structural study of the effect of mineral additives on the transparency, stability and ageing of silicate gels

N. El Felss[1], A. Gharzouni[1], M. Colas[1], J. Cornette[1], I. Sobrados[2] and S. Rossignol[1]

[1] Institut de Recherche sur les Céramiques (IRCER), 12 rue Atlantis, 87068 Limoges Cedex, France.

[2] Instituto de Ciencia de Materiales de Madrid, Consejo Superior de Investigaciones Científicas (CSIC), C/Sor Juana Inés de la Cruz, 3, 28049 Madrid, Spain

■ Corresponding author: sylvie.rossignol@unilim.fr, tel.: 33 5 87 50 25 64

Abstract

The objective of this work is to evaluate to structural evolution of silicate gel in function of time and mineral additives. A comparison between fresh and aged silicate gel synthesized by silica and potassium hydroxide was carried out using FTIR, Raman and ^{29}Si MAS-NMR spectroscopies. Then, different additives such as NaOH, AlOOH, $Li_2B_4O_7$ and HCl were incorporated in the silica solution. Their effect on the aspect, transparency, Q^n polymerization and stability of silicate gels was studied. The structural study has shown that the quantification of Q^n species is difficult using FTIR and Raman spectroscopy because of the existence of several contributions in the same spectral region of silicate species. More precise informations were given by ^{29}Si NMR spectroscopy which has demonstrated the increase of Q^3 species in the detriment of Q^4 revealing the depolymerization of the structure over time. The study of effect of additives reveals that HCl, AlOOH and $Li_2B_4O_7$ do not permit to improve the stability of the gel due to the formation of several networks. However, promising results of stability and transparency were obtained using NaOH with a molar ratio of former to modifier of 2.52.

Keywords: silicate, ^{29}Si MAS-NMR, Q^n, mineral additive, ageing, pH value

I. INTRODUCTION

Silicate gel has attractive properties such as transparency, high adsorption capacity [1] acid/base properties, insolubility in different solvents and thermal stability. Due to these properties, they can be used in several applications fields such as optical sensors and biosensors [2], for the removal of heavy metals from low content effluents [3], or high concentrations of toluene vapor from gas [4], in pharmaceutical industry [5].

Among the processes used to synthesize silica gels, there is sol-gel process [6], acidification or precipitation of silica [7, 8] and ion exchange in an alkaline solution [9,10].Whatever the used process, it is important to elucidate the

structure and the stability of the gel over time. The focus on the use of mineral precursors (silica and alkaline solution) due to their lower environmental impact [11] is important as well as the interaction of the silica with alkaline cations which was extensively studied. Different spectroscopic techniques such as nuclear magnetic resonance ^{29}Si NMR, infrared Fourier transform spectroscopy (FTIR), and Raman spectroscopy were used. The network connectivity is generally denoted by the structural unit Q^n, defined by Engelhard [12], with Q representing the silicon atom connected with n bridging oxygen atoms and (4-n) non-bridging oxygen atoms in a tetrahedral environment. The characterization of silicate solutions by ^{29}Si NMR allows the distinction and the quantification of the silicate species. The variation of the Q^n species depends on the Si/M ratio (with M = Na or/and K) and the pH value [13, 14]. It has been shown that the alkali silicate solution depolymerizes in the presence of cyclic species Q^{2c} and Q^{3c} thus indicating the formation of rings within the solution [15]. FTIR spectroscopic measurements indicate information on OH bonds [16,17] and SiO_2 framework characteristic of the asymmetric stretching vibration of Si–O–Si bond which are located between 1200 and 1000 cm^{-1} [18]. The silicate species Q^4, Q^3 and Q^2 are located respectively around 1150-1200, 1100 and 1000-1030 cm^{-1}, while the position of the species Q^1, Q^0 is respectively around 900-920 and 820-876 cm^{-1} [19]. Raman spectroscopy allows highlighting the depolymerization of the different species as a function of the content of alkaline ions [20,21]. Raman spectroscopy was also combined to chemometric techniques to easily determine the alkaline silicate solution depolymerization degree and therefore reactivity through the chains to rings ratio [22]. It was also used to study the Q^n speciation in binary potassium silicate melts [23]. The ageing of silicate gel is an important parameter to control because it influences the properties and thus the desired application. In fact, it was demonstrated that with time the condensation continues after gelation due to the high amount of labile hydroxyl groups. In addition to that, the polymerization reaction strengthens the network [24]. Wijnen et al [25], have studied silica gel after 1 year of ageing using ^{29}Si MAS-NMR. They have found a decrease of Q^3 species at the expense of Q^4.

Different additives can be added to silicate gel such as organic additives, gelatin, poly- vinyl alcohol and glycerol [26]. Furthermore, formamide and oxalic acid were proven to improve the strength of the gel, in order to resist to capillary stresses. However, few studies have investigated the addition of mineral additives. For example, inorganic salts were proven to affect the particle growth and the gel structure. Their influence was intimately related to the valency of the cation of the salt [27]. The additives added to silica can act as modifiers and /or formers [28] (polyhedra, connected by bridging oxygen atoms and located at the vertices). The network modifier cations are alkaline or alkaline earth, which lead to breaking the bridges between the different forming cations inducing negatively charged non-bridging oxygens. The use of modifier cations leads mainly to the increase of the NBO

(number of non-bridging oxygen atoms) and therefore to the depolymerization of the network. The effect of network-modifying cations on Q^n distributions depends on the alkali size. For example, in borosilicate glasses, it was demonstrated using Raman spectroscopy that the silica polymerization rate, defined as $(4Q^4+3Q^3+2Q^2+Q^1)/4$, increased with the increase of the ionic radius increase (Li< Na< K <Cs) [29]. Moreover, the increase of the amount of B^{IV} compared to B^{III} leads to the increase of the non-bridging oxygen (NBO) [30]. NMR spectroscopy study of B_2O_3 doped bioactive glasses synthesized with a sol-gel process reveals that the majority of the borate is present as anionic $BO_{4/2}^-$ species and the need for charge compensation leads to an increase of the polymerization degree of phosphate species [31]. Furthermore, FTIR spectroscopy on Al^{3+} doped silica gel adsorbents evidences the formation of Si-O-Al band situated at 960 cm^{-1} [32]. Otherwise, it has been shown that the addition of Al_2O_3 to the SiO_2 gel allows avoiding the dependence of glass transition temperature (T_g) on hydroxyl concentration. This effect is due to the highly cross-linked structure in alumina-silica gels [33].Indeed, previous studies confirm by NMR spectroscopy the formation of the chemical bond Si-O-Al in alumina-silica gels rather than Al-O-Al linking with Al_2O_3 content lower than 14 mol% [34]. Lithium silicate gels were also studied. The NMR results indicate that depending on the lithium source, the lithium ions can be part of the silica network or in the form of hydrated ions situated in the pores of the gel [35]. It was also demonstrated that the large size of hydration sphere of Li reduces its depolymerizing effect [36]. The structure of silicate gel is also modified by the presence of sodium. Low SiO_2/Na_2O molar ratio increases the NBO and favors the formation of Q^2 and Q^1 species in the form of chains, dimers, and monomers. However, high SiO_2/Na_2O molar ratio decreases the NBO and leads to structures consisting of Q^3 and Q^4 species. Furthermore, the hydrolytic stability and the compressive strength of sodium silicate gels were improved with the increase of SiO_2/Na_2O molar ratio [37]. Despite the numerous studies on the structure of silicate gel, there is a lack of informations on the relation between the structure evolution and the stability of the gel over the time and the role of mineral additives.

The aim of this work is to improve the stability of silicate gels. For this, the structural evolution of fresh and aged silicate gels was determined using several spectroscopic techniques (FTIR, Raman and ^{29}Si MAS-NMR). Then, the effect of different additives as NaOH, AlOOH, $Li_2B_4O_7$ and HCl on the transparency and the stability of the silicate gels was investigated.

II. EXPERIMENTAL PART

Synthesis of silicate gels

The synthesis of silicate gels was carried out using a rotary evaporator. A colloidal silica SiO_2 is placed in a flask and then mixed with potassium hydroxide. Then the whole mixture was matured for 30 min at 60 °C. In order

to avoid the formation of bubbles, the mixture was degassed for 1h at room temperature. The solution is then transferred into a vial and dried at 90 °C for 48 h. The recipient should be kept closed during the curing of the gel. In order to improve the silicate gel stability, different additives such as sodium hydroxide (NaOH), boehmite (AlOOH), lithium tetraborate ($Li_2B_4O_7$) and HCl were added to silica solution. The purity of the different precursors is presented in **Table 1.**

The initial synthesized silicate gel was denoted as G and the modified gels were denoted as G^x with x is NaOH or AlOOH or $Li_2B_4O_7$ or HCl.

Characterization techniques

FTIR spectra of the gels after curing were obtained on a Thermo Fisher Scientific 380 infrared spectrometer (Nicolet) using transparent potassium bromide (KBr). The IR spectra were collected between 4000 and 400 cm^{-1} with a resolution of 4 cm^{-1} and 64 scans. The atmospheric CO_2 contribution was removed via a straight-line fit between 2400 and 2280 cm^{-1}. All data was normalized by the most intense band Q^3.

^{29}Si MAS-NMR spectra of silicate gels were recorded with an AVANCE-400 Bruker spectrometer (9.4T magnetic field) working at 79.5 MHz. Spectra were recorded, after 5.0 μs irradiation with the MAS technique (5 kHz rotation around an axis inclined 54°44′ with respect the external magnetic field). The number of scans was 400. The time between acquisitions was set to 10 s to minimize saturation effects. The position of NMR components was referred to TMS. The fitting of NMR spectra was performed with the dmfit software (D. Massiot, CNRS), that allowed position, linewidth and intensity of components to be deduced with a nonlinear least-square iterative method. The errors for chemical shifts and relative area are estimated at 0.2 ppm and 2% respectively.

The Raman spectra were acquired using an inVia Reflex Renishaw confocal Raman spectrometer. Raman data were collected with 532 nm laser operating on the gel at a power of 40 mW. The objective used was x100 with a holographic grating of 2400 lines/mm. The spectral rage was 700 to 1200 cm^{-1}, and the acquisition time was 2 accumulations of 60 s.

UV spectroscopy was performed on the gel using a CARY 5000 spectrophotometer. The spectra were obtained between 400 and 750 nm with a baseline set to 0 and a step of 1 nm.

The pH values were measured after the synthesis of the gels using a Schott Instrument Lab860 pH-meter at 25°C.

The stability of gels depends on their irreversible state. In order to verify this, the vials containing the gels are placed upside down in an oven at around 50 °C. A graduation is pasted on the vials in order to follow the deformation of the meniscus of the gel as a function of time.

III. RESULTS AND DISCUSSION

1. Structure evolution of gels

The structural characterization of silicate gel was carried out using FTIR and ^{29}Si MAS NMR spectroscopies. The **Fig. 1** presents FTIR, ^{29}Si MAS NMR and Raman spectra of silicate gel before and after ageing. The bands and their assignments are detailed in **Table 2**. The different bands related to the different contributions of the species present in silicate gel before ageing (**Fig. 1-A-a)** are identifiable such as $\nu(OH)$ and $\delta(OH)$ located at 3300 and 1650 cm^{-1}, they are attributed respectively to the OH stretching vibration and bending vibration of water molecules [38]. The bands attributed to C-H stretching ($\nu(CH)$) and bending ($\delta(CH)$) vibrations are respectively at 2900, and 1460 cm^{-1} [39]. The vibration bands of Si–O–Si bond are located between 1250 and 800 cm^{-1} [40]. Indeed, the siliceous species Q^4, Q^3, Q^2 characteristic of the asymmetric stretching vibrations of Si-O-Si are respectively at 1143, 1038 and 953 cm^{-1} [41]. The Q^1 contribution appears at 866 cm^{-1} [41]. After ageing (**Fig. 1-A-b**), no significant change was observed in the Q^n bands as mentioned on **Table 2**, expect for the intensities of the $\nu(OH)$ and $\nu(CH)$ bands which decrease after ageing. An example of deconvolution of ^{29}Si NMR spectrum of the studied silicate gel before ageing is given in **Fig. 1-B-a'**. Broad bands of Q^4 and $Si(OH)_4$ are detected at -107 and -110 ppm respectively with a total percentage area of 16 and 2 %. It is also noted the predominance of Q^3 species with two components at -97 and -99 ppm and a total percentage area of 54%. Cyclic species Q^{3c} and Q^{2c} can be distinguished at -90 and -81 ppm [42] with a low percentage area of 7 and 1 %. Q^2 and Q^1 species are observed at -88 and -80 ppm with a percentage area of 14 and 3 %, respectively. Indeed, the cyclic contributions Q^{2c} and Q^{3c} are not identified by FTIR spectroscopy, they are only quantifiable by NMR spectroscopy. No Q^0 can be detected. These assignments are in accordance with literature [43,44]. The predominance of Q^4 and Q^3 species reveals that the gel is mainly composed of highly polymerized and condensed silicate species. For the ^{29}Si NMR spectrum of gel after ageing (**Fig. 1-B-b'-b**), all the chemical shifts are the same as those observed on the gel before ageing, except for the species Q^4 and Q^{3c} which are receptively at -106 and -89 ppm with a total percentage area of 10 and 6 %. Other variations in the areas of Q^n species are observed, especially at Q^3 and Q^1 levels as mentioned on the **Table 2**, which are 57 and 2 %. For the full width at half maximum presented on the **Table 2**, no difference was observed before and after ageing at Q^1, Q^2, Q^{2c} and Q^{3c} levels. A slight variation was observed on Q^4 and Q^3 species, it was respectively 4.50, 3.63 ppm before ageing, 3.14, and 3.78 ppm after ageing.

An example of deconvolution of Raman spectrum of the silicate gel before ageing is presented in **Fig. 1-C-c'**. The bands located at 754 and 788-821 cm^{-1} are assigned respectively to the stretching vibration of C-N band and

CH$_2$ rocking mode [45][46]. The assignment of Raman bands is complicated to attribute in the frequency range 900-1200 cm^{-1} due to the overlap of different vibrations. Indeed, many vibrations are coupled. The different bands are attributed to the COH deformation (1342 cm^{-1}), CCO vibration modes (1054 and 1115 cm^{-1}) and CH$_2$ rocks (976 and 925 cm^{-1}) [47]. These vibrations are due to the other organic components of the silicate gel. The bands Q^4 and Q^1 species are located respectively at 1110 and 855 cm^{-1} with percentage area of 1 and 3 % [48] [49]. The contributions of species Q^3 and Q^{3c} are observed respectively at 1045 and 1010 cm^{-1} with 28 and 8 % as an area percentage [50]. Low area percentages are observed for the species Q^2 and Q^{2c} located at 952 and 910 cm^{-1}, they are respectively 1 and 0 % [51]. No Q^0 was detected. These assignments are in accordance with literature. However, the overlap of these different contributions may false the decomposition of the spectra and therefore the area percentages of the Q^n species, especially for species Q^2, Q^3 and Q^{3c}. After ageing **(Fig. 1-C-d'-b),** the area percentage of Q^4 species located at 1097 cm^{-1} increased to 4 %. The same variations observed for species Q^{3c}, Q^{2c} located respectively at 1015 and 905 cm^{-1} with area percentages of 13 and 1 %. A decrease in the area percentages is observed for the species Q^3, Q^2 and Q^1 located respectively at 1047, 952 and 853 cm^{-1} as mentioned on the **Table 2,** which are 1, 1 and 2%.

In order to understand the structural changes after aging, all the percentages of intensities and areas were presented according to the species Q^n. The FTIR intensity of each Q^n unit was normalized with compared to the sum of all the intensities of the Q^n species and then reduced to 100%. The **Fig. 2** shows the percentages of Q^n intensity calculated by FTIR spectroscopy and the percentages of Q^n area calculated by ^{29}Si NMR spectroscopy of the silicate gel before and after ageing. The intensity percentages (**Fig. 2 2-A**) of the species Q^4, Q^3 Q^2 Q^1 before ageing are 25, 41, 23 and 11 % respectively. However, after ageing, a slight variation on the intensity percentages is observed at the levels of Q^4 and Q^1, they are 26 and 10 %. For the rest of the species no change was observed. The intensity ratio Q^4/Q^3 is 0.60 before ageing and 0.63 after ageing. This slight evolution is not enough to conclude on the evolution of silicate species after ageing. More complementary and quantitative information is given by ^{29}Si NMR spectroscopy. The values of the percentages of area of the Q^n species obtained by ^{29}Si NMR spectroscopy are presented on **Fig. 2 2-B**. As mentioned on the **Table 2**, some variations are observed after ageing. The area ratio Q^4/Q^3 is 0.29 before ageing and 0.17 after ageing. This means that a depolymerization of Q^n species occurs over time. This is not in accordance with literature showing the formation of higher order silicate species and therefore the polymerization of the structure over time [52,53]. This can explain the non-stability of this gel. The values of the percentages of area of the Q^n species obtained by Raman spectroscopy are presented on **Fig. 2-C**. The area ratio Q^4/Q^3 is 0.04 before ageing and 0.18 after ageing. This is not in accordance with the results obtained

by ^{29}Si NMR spectroscopy. Indeed, the measurements by silicon NMR are specific only to the siliceous species Q^n, while by Raman spectroscopy, other contributions associated with the C-N, C-C and CH_2 bonds are also observed in the same frequency range as that of the Q^n species, namely between 800 and 1200 cm^{-1}. The area percentages obtained by Raman spectroscopy are not specific to Q^n species. Although Raman spectroscopy is a powerful technique, it can not be used in this case to quantify the Q^n species because of the contributions of the other components of silicate gel. Only ^{29}Si NMR spectroscopy is selective for the Q^n species present in the gel.

In order to improve the stability of the gel, different additives were added and their impact on Q^n species distribution was studied.

2. Influence of additives on Q^n polymerization

The influence of the chemical composition of the additives on the silica was evaluated by carrying out various reaction mixtures. The amount of moles of alkaline was varied compared to that of the initial gel which is 0.23 mol. The additives added to silica can act as modifiers and /or formers as explained in the introduction.

Feature and pH value

Table 3 presents the photographs of the gels obtained after curing. All the gels obtained have a solid texture. The appearance of the gels differs depending on the additive added. The gels produced with $Li_2B_4O_7$ and HCl have a white appearance. The use of AlOOH modifes slightly the gels with a cloudy and less white appearance. The initial gel as well as the gel modified with NaOH have a transparent appearance. The pH values were measured directly after the synthesis of the gels. The pH values of all the modified gels are presented in **Table 4**. For the initial gel noted G, the pH value is 12.14. After adding NaOH, AlOOH, $Li_2B_4O_7$ and HCl, the pH values decrease to 11.5, 11.89, 11.80 and 11.70 respectively. This decrease in pH value compared to the reference means a variation in the level of Q^n species able of polycondensation reactions. Goto demonstrated that polymerization is favored and larger particles are formed at higher pH [54]. However, the formation and polymerization of silicate gels with a basic pH value higher than 10 is not much studied in literature.

FTIR results

The FTIR spectra are recorded at 20 °C and after 1 hour of reactive mixture stirring. **Fig. 3** shows the FTIR spectra of the silica mixed with KOH, NaOH, AlOOH, $Li_2B_4O_7$ and HCl. In **Fig. 3** the spectrum of the reference mixture with KOH (a) indicates that the Q^4 species is located at 1175 cm^{-1}. When adding the additives NaOH (spectrum (b)), AlOOH (spectrum (c)), $Li_2B_4O_7$ (spectrum (d)) and HCl (spectrum (e)) the positions of the species

Q^4 are slightly shifted to lower wavenumbers, except for NaOH. Indeed the positions of Q^4 with AlOOH, $Li_2B_4O_7$ and HCl are respectively at 1169, 1167 and 1163 cm^{-1}, while the mixture with NaOH indicates a position of the Q^4 species, which is at 1180 cm^{-1}. No significate variation is observed on the positions of Q^2 and Q^3 species after adding all the additives. For example, the positions of Q^2 and Q^3 species after addition of NaOH are respectively 998 and 1103 cm^{-1} relative to those of the initial mixture with only KOH which are at 989 and 1099 cm^{-1} ($\pm$ 4 cm^{-1}). The difference towards the higher wavenumbers with NaOH compared to the reference of the Q^n species is significant of a slight polymerization of the siliceous species, while the shift towards the lower wavenumbers with the other additives indicates a depolymerization of the siliceous species.

The positions of the Q^4 species were noted on all of the FTIR spectra of the produced gels. The Q^4 positions of the gel (Si + KOH) were chosen as a reference. **Fig. 4** shows the values of the $Q^4/Q^{4\,ref}$ ratios as a function of Si/ΣM molar ratios. This latter represents the molar ratio $n^{silicon} : n^{modifier\ additives}$. The choice of the modifier elements (Li, Al, Na, K) can be explained by their capacity to influence the nature of silicate species as explained in introduction part. A Q^4/Q^{4ref} ratio equal to or higher than 1 means that the associated mixture is likely to have a polymerization effect on the gels with positions of Q^n species located in the direction of the polymerization in comparison with the chosen reference. The first step in selecting potential additives capable of improving the stability of the gels was to eliminate $Q^4/Q^{4\,ref}$ values less than 1 and associated with high Si/ΣM ratios. These mixtures are associated to the formulations containing the additives based on AlOOH, HCL and $Li_2B_4O_7$ with molar ratios Si/ΣM of 11.40, 11.80 or 23.75 and 12.13 or 24.78 respectively. These additive rates are not expected to have a polymerizing effect in the gels. The second step consisted in focusing on the range of Si/ΣM molar ratios between 1.67 and 4.96 and eliminating $Q^4/Q^{4\,ref}$ values less than 1. After these two selection, the mixtures which are likely to have a polymerizing effect are those with KOH (reference mixture), $Li_2B_4O_7$ and NaOH. Their respective molar ratios are 2.48, 2.25, 2.52 and their values of $Q^4/Q^{4\,ref}$ ratios are equal or higher than 1. These data allow concluding on a range of molar ratio inducing a polymerization of the siliceous species Q^3 that must be equal and/or less than 2.52.

Transparency of gels

Transmittance measurements were carried out by ultraviolet-visible spectroscopy (400 nm-750 nm) in order to determine the transparency degree of the gels after curing. The transmittance curves of the modified gels are presented in **Fig. 5**. The transparency of the initial reference gel (**Fig. 5-(a)**) is 81%. The gel modified with NaOH

(**Fig. 5- (b)**) indicates a percentage of transmission of 69 %. After adding AlOOH (**Fig. 5- (c)**), the transparency is 5%. A gel with 0% transparency is obtained with the additive $Li_2B_4O_7$ (**Fig. 5- (d)**).

The only additive allowing to obtain a high transparency as the initial gel without additives is sodium hydroxide (NaOH). This composition has an Si/ΣM molar ratio of 2.52 and a pH value of 11.5. This mixture becomes very viscous even before the maturation stage. This may be due to the fast gelation of the sol, thus leading to small particle sizes. Indeed, it has been observed with the use of Na_2SiO_3 as a molar ratio $H_2O : Na_2SiO_3$ at 0.38 that the decrease in particle size can be explained by a high condensation rate of main particles which leads to a higher number of silica species with reduced size. The smaller the particle size, the greater the degree of transparency of the gels [55]. The more the pH value decreases towards values, which remain, higher than 10, the more the size of the particles decreases and the transparency of silicate gels increases.

Stability of silicate gels

The synthesized gels having a transparency between 5 and 81% were placed upside down in an oven at 50 °C in order to follow their ageing over the time. **Fig. 6** presents the values of meniscus progression of the different gels as a function of the time. The initial silicate gel without additives tends to creep after 6 days reaching 100% of the height of the initial gel. For the gel modified with NaOH, the progression of the meniscus is very low and does not exceed 19% of the height of the initial gel after 50 days at 50 °C. This measurement has been repeated and still presents the same result. The same creep behavior of the initial gel with KOH is observed on the modified gels with AlOOH and $Li_2B_4O_7$, which also creep after 6 days. This may be due to the formation of the Si-O-Al and Si-O-B bonds corresponding to Q^2 or Q^1 species. In the case of the initial gel, the KOH is a network modifier which breaks the bonds between the condensed silicon species generating non-bridging oxygen atoms. The AlOOH can be dissolved to form $Al(OH)_4^-$ [56]. The resulting aluminium can react with silicate species leading to the formation of different networks. Similarly to glasses and geopolymers [29, 57], the boron from lithium tetraborate (asymmetric B^{III}) leads to the appearance of non bridging oxygens, resulting in charge defects in the structure. So, boron interacts with the alkali cation in the silicate gel to compensate this charge defects. Si-O-B bonds can also be formed. Consequently, there is formation of several networks in the resulting gel.

In order to understand the ageing behavior with sodium hydroxide (NaOH) which seems stabilizing the initial silicate gel over the time, the structure of the gel was studied by FTIR spectroscopy. **Fig. 7** shows the intensity percentages of the different Q^n species present in silicate gel before and after adding NaOH. The intensity percentages of the species Q^4, Q^3, Q^2 and Q^1 of the initial gel are 25, 39, 23 and 12%. Whereas after addition of NaOH, the intensity percentages are respectively 32, 38, 21, 7%. A slight variation is observed at the level of the

species Q^3 and Q^2. However, it is observed the increase in Q^4 species and the decrease in Q^1 species for the gel modified with NaOH. The intensity ratio Q^4/Q^3 is 0.64 in the initial gel and 0.84 after adding NaOH. This evolution after adding NaOH suggest the formation of higher order silicate species and therefore the polymerization of the structure [53, 52].

It would seem relevant to focus on controlling the minimum pH values, to control the transparency (around 69 %) and to have molar ratios between 2.48 and 2.52 in order to stabilize alkali-based silicate gels.

IV. CONCLUSION

This work aims to improve the stability of silicate gels. For this, a silicate gel based on based silica and potassium hydroxide with various additives were investigated and characterized after synthesis and after ageing using different spectroscopic techniques (FTIR, Raman and ^{29}Si MAS-NMR spectroscopies).

The structural study of the initial gel by FTIR and ^{29}Si MAS-NMR spectroscopies demonstrated the decrease of Q^4/Q^3 area ratio after ageing revealing the depolymerization of the structure over time. In order to improve the stability of the gel, different additives (NaOH, AlOOH, $Li_2B_4O_7$ and HCl) were added and their impact on the transparency, the stability and Q^n species distribution was studied. The transparency was very reduced by HCl, AlOOH and $Li_2B_4O_7$. However, NaOH preserves the transparency of gel. The ageing was accelerated by placing the silicate gels at 50 °C. The silicate gel without additives tends to creep after 6 days. The gels with AlOOH and $Li_2B_4O_7$ exhibit the same behavior due to the formation of the Si-O-Al and Si-O-B bonds inducing the formation of several networks. However, it is possible to stabilize the gel ageing by adding NaOH ($n_{Si}/(n_{Na}+n_K) = 2.52$) due to the polymerization of siliceous species.

V. REFERENCES

[1] Nasri Z, Shams E (2009) Application of silica gel as an effective modifier for the voltammetric determination of dopamine in the presence of ascorbic acid and uric acid. Electrochimica Acta 54:7416-7421

[2] Estella J, Echeverría J, Laguna M, Garrido J (2007) Effects of aging and drying conditions on the structural and textural properties of silica gels. Microporous Mesoporous Mater 102:274-282

[3] Guibal E, Lorenzelli R, Vincent T, Cloirec P (2010) Application of Silica Gel to Metal Ion Sorption: Static and Dynamic Removal of Uranyl Ions. Environ Technol 16:101-114

[4] Sui H, Liu H, An P, He L, Li X, Cong S (2017) Application of silica gel in removing high concentrations toluene vapor by adsorption and desorption process. J Taiwan Inst Chem E 74:218-224

[5] Hentzschel M, Alnaief M, Smirnova I, Sakmann A, Leopold CS (2012) Tableting properties of silica aerogel and other silicates. Drug Dev Ind Pharm 38:462–467

[6] Livage J, Henry M, Sanchez C (1988) Sol-gel chemistry of transition metal oxides. Prog Solid St Chem 18: 259-341

[7] Vail JG (1952) Soluble silicates: Their properties and uses. Reinhold, New York, 1:357

[8] McGavack J, Patrick WA (1920) The adsorption of sulfur dioxide by the gel of silicic acid. J Am Chem Soc 42:946-978

[9] Gerber T, Himmel B, Hübert C (1994) WAXS and SAXS investigation of structure formation of gels from sodium water glass. J Non Cryst Solids 175:160-168

[10] Lee CJ, Kim GS, Hyun S.H (2002) Synthesis of silica aerogels from waterglass via new modified ambient drying. J Mater Sci 37:2237-2241

[11] Dokkum V, Hulskotte HP, Kramer JHJ, KJM Wilmot (2004) Emission, fate and effects of soluble silicates (waterglass) in the aquatic environment. Environ Sci Technol 38:515–521

[12] Engelhard G, Zeigan D, Jancke H, Hoebbel D, Weiker Z (1975) High resolution ^{29}Si NMR of silicates and Zeolites. Anorg Allg Chem 418:17–28

[13] Brykov AS, Danilov VV, Yu Aleshunina E (2008) State of silicon in silicate and silica-containing solutions and their binding properties. Russ J Appl Chem 81:1717–1721

[14] Tognonvi MT, Soro J, Rossignol S (2012) Physical-chemistry of silica/alkaline silicate interactions during consolidation. Part 2: effect of pH. J Non Cryst Solids 358:492-501

[15] Svensson L, Sjöberg S, Öhman LO (1986) Polysilicate equilibria in concentrated sodium silicate solutions. J Chem Soc Faraday Trans. 1 82:3635–3646

[16] Cannas C, Casu M, Musinu A, Piccaluga G (2005) 29Si CP MAS NMR and Near-IR study of sol-gel microporous silica with tunable surface area. J Non Cryst Solids 351:34-76

[17] Estella J, Echeverria JC, Laguna M, Garrido J (2007) Effect of supercritical drying conditions in ethanol on the structural and textural properties of silica aerogels. Microporous Mesoporous Mater 102-274

[18] Lutz W, Täschner D, Kurzhals R, Heidemann D, Hübert C (2009) Characterization of Silica Gels by 29Si MAS NMR and IR Spectroscopic Measurements. Z. Anorg Allg Chem 2191-2196

[19] MacDonald SA, Schardt CR, Masiello DJ, Simmons JH (2000) Dispersion analysis of FTIR reflection measurements in silicate glasses. J Non Cryst Solids 275:72-82

[20] Mysen BO, Cody GD (2005) Solution mechanisms of H$_2$O in depolymerized peralkaline melts. Geochim. Cosmochim 69:5557-5566

[21] Vidal L, Gharzouni A, Joussein E, Colas M, Cornette J, Absi J, Rossignol S (2017) Determination of the polymerization degree of various alkaline solutions: Raman investigation. J Sol-Gel Sci Technol 83:1-11

[22] Arnoult M, Dupuy C, Colas M, Cornette J, Duponchel L, Rossignol S (2019) Determination of the Reactivity Degree of Various Alkaline Solutions: A Chemometric Investigation. Applied Spectroscopy, 73:12

[23] Malfait WJ, Zakaznova-Herzog VP, Halter WE (2007) Quantitative Raman spectroscopy: High-temperature speciation of potassium silicate melts. J Non Cryst Solids 353:4029-4042

[24] Kalapathy U, Proctor A, Shultz J (2000) Production and properties of flexible sodium silicate films from rice hull ash silica. Bioresour Technol 72:99-106

[25] Wijnen PWJG, Beelen TPM, Rummens KPJ, Saeijs HCPL, De Haan JW, Van De Ven LJM, Van Santen RA (1991) The molecular basis of aging of aqueous silica gel. J Colloid Interf Sci 145:17-32

[26] Nassif N, Roux C, Coradin T, MN Rager, OMM Bouvet, Livage JA (2003) Sol-gel matrix to preserve the viability of encapsulated bacteria. J Mater Chem. 13 203–208

[27] Murakata T, Sato S, Ohgawara T (1992) Control of pore size distribution of silica gel through sol-gel process using inorganic salts and surfactants as additives. J Mater Sci 27:1567-1574

[28] Jiang ZH, Zhang QY (2014) The structure of glass: a phase equilibrium approach. Prog Mater Sci 61:144-215

[29] Neyret M, Lenoir M, Granhean A, Massoni N, Penelon B, Malki M (2015) Ionic transport of alkali in borosilicate glass. Role of alkali nature on glass structure and on ionic conductivity at the glassy state, J Non Cryst Solids 410:74-81

[30] Xie J, Tang H, Wang J, Wu M, Han J, Liu C (2018) Network connectivity and properties of non-alkali aluminoborosilicate glasses. J Non Cryst Solids 481 :403-408

[31] Deilmann L, Winter O, Cerrutti B, Bradtmüller H, Herzig C, Limbeck A, Lahayne O, Hellmich C, Eckert H, Eder D (2020) Effect of boron incorporation on the bioactivity, structure, and mechanical properties of ordered mesoporous bioactive glasses. Mater Chem B 8:1456

[32] Fang YT, Liu T, Zhang ZC, Gao XN (2014) Silica gel adsorbents doped with Al, Ti, and Co ions improved adsorption capacity, thermal stability and aging resistance. Renew Energy 63:755-761

[33] Liu S, Boffa V, Yang D, Fan Z, Meng F, Yue Y (2018) Clarifying the gel-to-glass transformation in Al$_2$O$_3$-SiO$_2$ systems. J Non Cryst Solids 492:77‑83

[34] Ren JJ, Zhang L, Eckert H (2014) Medium-range order in sol–gel prepared Al2O3–SiO2glasses: new results from solid-state NMR. J Phys Chem C 118:4906–4917

[35] Szu SP, Klein LC, Greenblatt M (1990) Effect of precursors on lithium containing silicate gels studied by 7Li nuclear magnetic resonance. J Non Cryst Solids 121:1-3

11

[36] Schwartz I, Anderson P, de Lambilly H, Klein LC (1986) Stability of lithium silicate gels. J Non Cryst Solids 83:391-399

[37] D Dimas, I Giannopoulou, D Panias (2009) Polymerization in sodium silicate solutions: a fundamental process in geopolymerization technology. J Mater Sci 44:3719-3730

[38] M. Muroya (1999) Correlation between the formation of silica skeleton and Fourier transform reflection infrared absorption spectroscopy spectra. Colloid Surf A 157:147-55

[39] Chiang CH, Ishida H, Koenig JL (1980) The Structure of y-Aminopropyltriethoxysilane on Glass Surfaces. J Colloid Interf Sci 74:396-404

[40] Lutz W, Taschner D, Kurzhals R, Heidemann D, Hubert C (2009) Characterization of Silica Gels by ^{29}Si MAS NMR and IR Spectroscopic Measurements. Z Anorg Allg Chem 635:2191-2196

[41] Tan J, Zhao S, Wang W, Davies G, Mo X (2004) The effect of cooling rate on the structure of sodium silicate glass. Mater Sci Eng B 106:295-9

[42] Knight CTG (1988) A two-dimensional silicon-29 nuclear magnetic resonance spectroscopic study of the structure of the silicate anions present in an aqueous potassium silicate solution. J Chem Soc Dalton Trans. 1457-1460

[43] Kawazoe H, Application of NMR Spectroscopy to the Science and Technology of Glasses and Ceramics (1994) Editor(s): I. Ando, G.A. Webb, Annual Reports on NMR Spectroscopy, Academic Press, 28:1-27

[44] Sjöberg S (1996) Silica in aqueous environments. J. Non-Cryst. Solids 196:51-57

[45] Michaud PT, Babic D (1998) A Raman Study of Etching Silicon in Aqueous Tetramethylammonium Hydroxide. J Electrochem Soc 145:11

[46] Gryniewicz-Ruzicka C, Arzhantsev S, Pelster LN, Westenberger B, Buhse, J Kauffman (2011) Multivariate Calibration and Instrument Standardization for the Rapid Detection of Diethylene Glycol in Glycerien by Raman Spectroscopy. Appl Spectrosc 65:334-341

[47] Mendelovici E, Frost RL, Kloprogge T (2000) Cryogenic Raman spectroscopy of glycerol. J Raman Spectrosc 31:1121-1126

[48] Zotov N, Keppler H (1998) The influence of water on the structure of hydrous sodium tetrasilicate glasses. Am Mineral 83:823-834

[49] Matos MC, Ilharco LM, Almeida RM (1992) The evolution of TEOS to silica gel and glass by vibrational spectroscopy. J Non Cryst Solids 147-148:232-237

[50] Brykov AS, Danilov VV, Aleshunina EY (2008) State of silicon in silicate and silica-containing solutions and their binding properties. Russ J Appl Chem 81:1717-1721

[51] Melkior T, Yahiaoui S, Thoby D, Motellier S, Barthès V (2007) Diffusion coefficients of alkaline cations in Bure mudrock. Phys Chem Earth 32:453-462

[52] Goudarzi N (2013) Silicon-29 NMR spectroscopy study of the effect of tetraphenylammonium (TPA) as a template on distribution of silicate species on alkaline aqueous and alcoholic silicate solutions. Appl Magn Reson 44:469-78

[53] Vega AJ, Scherer GW (1989) Study of structural evolution of silica gel using ^{1}H and ^{29}Si NMR. J Non Cryst Solids 111:153-166

[54] Goto K (1956) Effect of pH on polymerization of silicic acid. J Phys Chem 60: 1007-1008

[55] Bangi UKH, Jung IK, Park CS, Baek S, Park HH (2013) Optically transparent silica aerogels based on sodium silicate by a two step sol–gel process and ambient pressure drying. Solid State Sci 18:50-57

[56] Panias D, Asimidis P, Paspaliaris I (2001) Solubility of boehmite in concentrated sodium hydroxide solutions: model development and assessment. Hydrometallurgy 59:15-29

[57] Dupuy C, Gharzouni A, Sobrados I, Texier-Mandoki N, Bourbon X, Rossignol S (2019) ^{29}Si, ^{27}Al, ^{31}P and ^{11}B magic angle spinning nuclear magnetic resonance study of the structural evolutions induced by the use of phosphor- and boron–based additives in geopolymer mixtures. J Non Cryst Solids 521:119-541

(A)
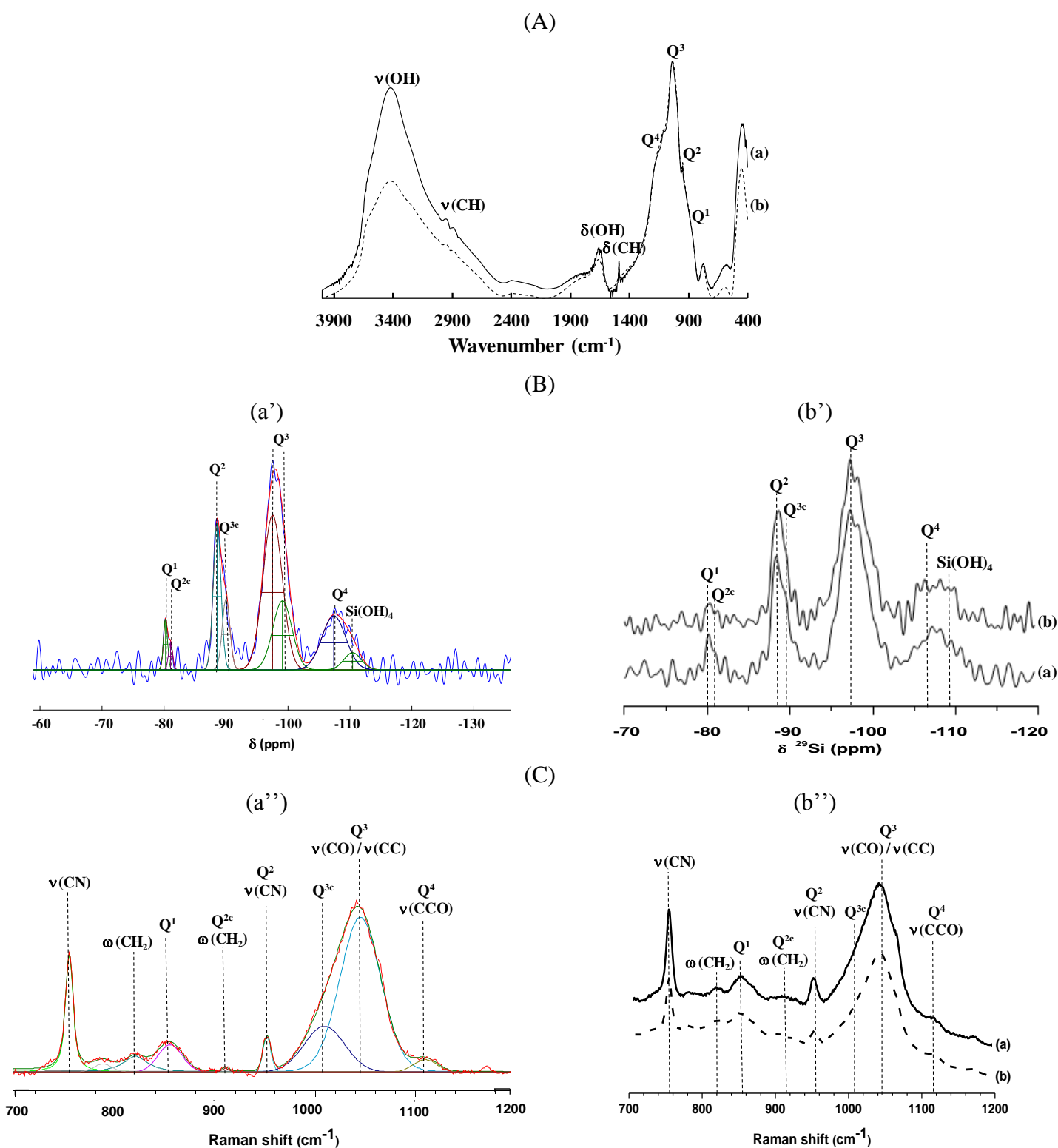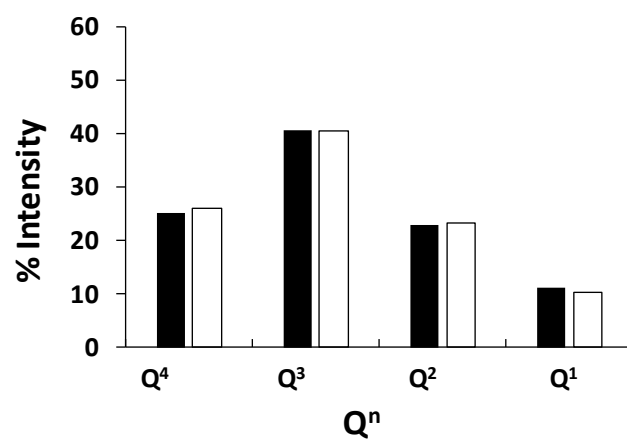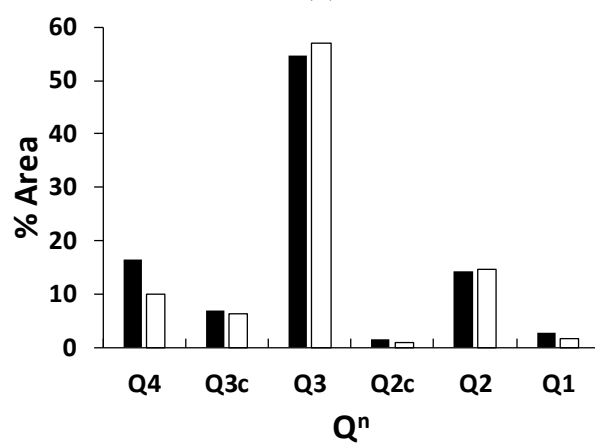
(B)

(a')

(b')

(C)

(a'')

(b'')

Fig. **Erreur ! Document principal seulement.** (A) FTIR, (B) ^{29}Si NMR spectra with (a') example of NMR deconvolution and (b') spectra of silicate gel (a) before and (b) after ageing and (C) Raman spectra with (a'') example of Raman deconvolution and (b'') spectra of silicate gel (a) before and (b) after ageing
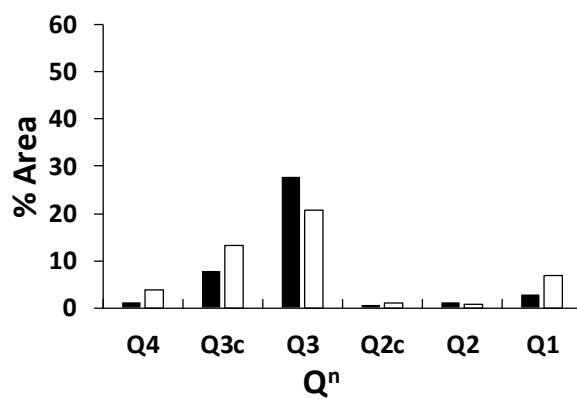
(a)

(b)

(c)

Fig. **Erreur ! Document principal seulement.** Percentages of (a) FTIR intensity, (b) ^{29}Si NMR area and (c) Raman area of the different Q^n species in silicate gel (■) before and (□) after ageing
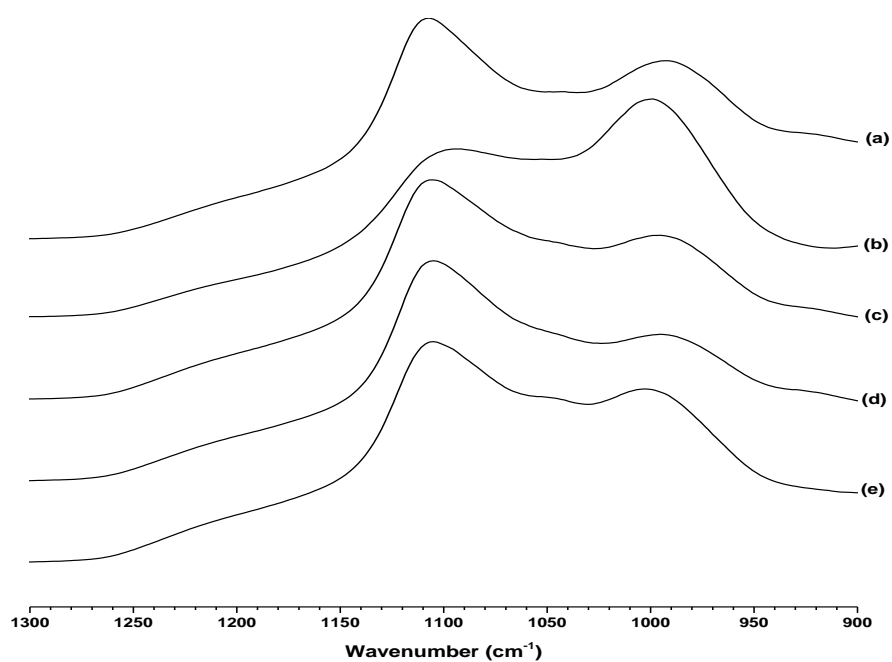
Fig. **Erreur ! Document principal seulement.** FTIR spectra of modified gels with (a) KOH, (b) NaOH, (c) AlOOH, (d) $Li_2B_4O_7$ and (e) HCl in the interval 1300-900 cm^{-1} at 20 °C after 1h under stirring
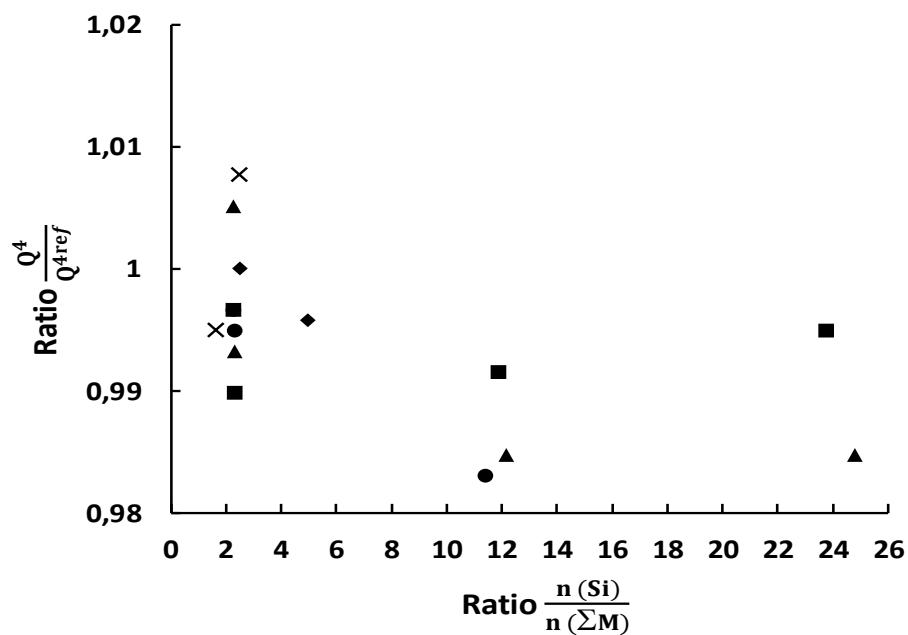

Fig. 4 Values of the ratio Q^4/Q^{4ref} as a function of the ratio $n(Si)/n(\Sigma M)$ of the silica mixtures with (◆)KOH, (●)NaOH, (■) AlOOH, (▲) $Li_2B_4O_7$ and (✗) HCl
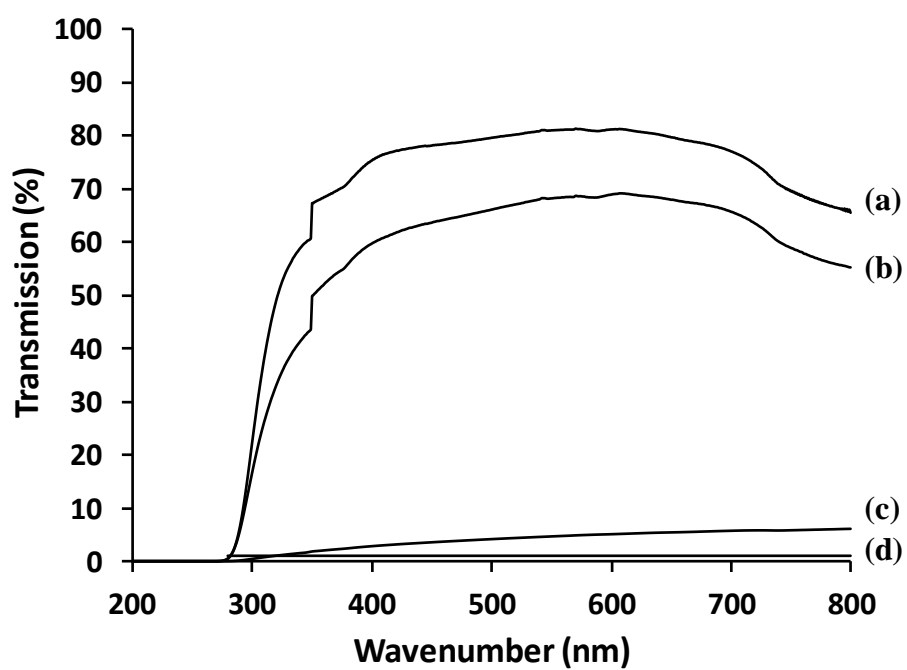
Fig. **Erreur ! Document principal seulement.** Transmission percentages of (a) silicate gel, silicate gel modified with (b) NaOH, (c) AlOOH and (d) $Li_2B_4O_7$
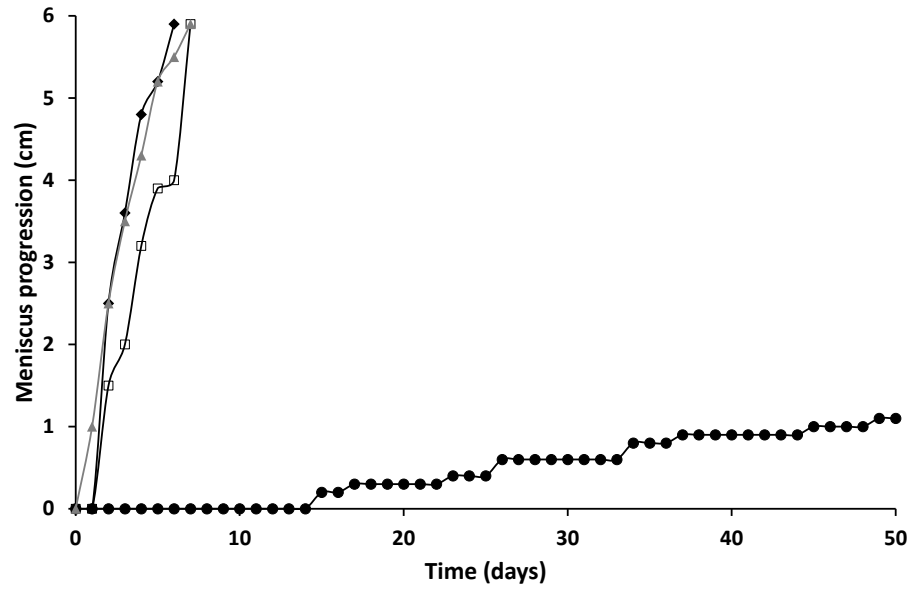
Fig. **Erreur ! Document principal seulement.** Meniscus progression of (◆) initial silicate gel and modified silicate gels with (●) NaOH, (■) AlOOH and (▲) $Li_2B_4O_7$
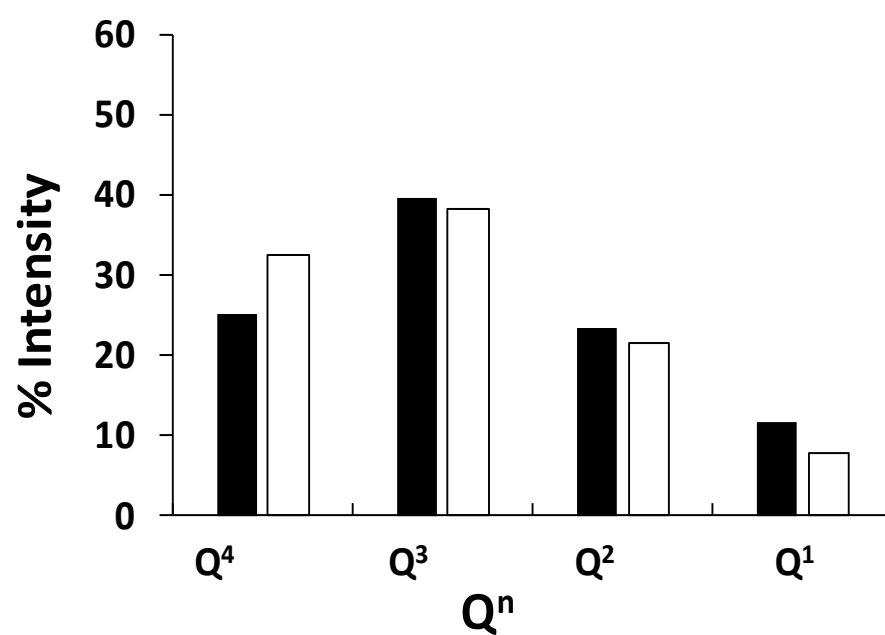
Fig. **Erreur ! Document principal seulement.** Percentages of FTIR intensity of the different Q^n species present in silicate gel (■) before and (□) after adding NaOH. The intensities were normalized to the total sum of Q^n intensities and reduced to 100%

Table Erreur ! Document principal seulement. **:** Purity percentages of the different precursors used

Precursors	SiO$_2$	KOH	NaOH	AlOOH	Li$_2$B$_4$O$_7$	HCl
Purity (%)	49.8	50.5	97	80	99.50	37
supplier	Merck Germany	Sigma-Aldrich USA	Sigma-Aldrich USA	Sasol USA	Sigma-Aldrich USA	VWR USA